

Performance evaluation for 160-Gb/s optical phase conjugation systems considering dispersion mapping and third-order dispersion

Jianqiang Li (李建强), Kun Xu (徐 坤), Guangtao Zhou (周光涛),
Jian Wu (伍 剑), and Jintong Lin (林金桐)

Key Laboratory of Optical Communication and Lightwave Technologies, Ministry of Education,
Beijing University of Posts and Telecommunications, Beijing 100876

Received August 9, 2006

The impact of third-order dispersion (TOD) is investigated by numerical simulations in 160-Gb/s single-channel systems incorporated with dispersion mapping and optical phase conjugation (OPC). System performances using retransmission-to-zero (RZ) or carrier-suppressed RZ (CSRZ) modulation format are evaluated on the optimized dispersion map. The results indicate that even though TOD has been fully compensated, the intra-channel nonlinearity induced by local TOD would degrade the system performance in nonlinear regime. The scheme with an optimized dispersion map provides a much higher performance and offers a larger tolerance on a variation of pre-compensation. CSRZ modulation format is more robust due to its tradeoff between tolerances on intra-channel nonlinearity and dispersion.

OCIS codes: 060.0060, 060.2360, 120.4820.

Optical phase conjugation (OPC) is known to be a good candidate to compensate dispersion^[1] and intra-channel nonlinearity^[2] in optical communication systems. But the major limitations of OPC are the requirements on the dispersion map and power profile. Recently, OPC combined with dispersion mapping in the pseudo-linear regime^[2] is effective for nonlinearity compensation alone regardless of the power profile. This scheme was experimentally achieved in 40-Gb/s systems^[2]. With the development of optical-time-division-multiplexing (OTDM) technique, increasing single channel bit-rate becomes available in wavelength division multiplexing (WDM) systems to reduce the number of channels. As the bit-rate increases to 100 Gb/s and beyond, the third-order dispersion (TOD), known as the dispersion slope, plays an important role in the transmission. However, the introduction of OPC cannot compensate the odd-order dispersion. Hence, the TOD accumulates along the transmission distance in high-speed OPC systems. Some TOD-compensating elements are necessary to be inserted in the link. Comprehensive investigations on TOD effects and performance evaluations in 160-Gb/s OPC systems employing dispersion mapping have not been done.

In this letter, the impact of TOD in 160-Gb/s OPC systems with dispersion mapping is discussed. Numerical simulations are used to assess the system performances employing RZ and CSRZ modulation formats.

Figure 1 is a schematic diagram of the system configuration in the simulation. The 160-Gb/s transmitter using $2^7 - 1$ pseudo-random bit sequence (PRBS) at 1550 nm generates such modulation formats as return-to-zero (RZ) with 33% duty cycle (RZ33), return-to-zero with 50% duty cycle (RZ50), and carrier-suppressed return-to-zero (CSRZ). At the receiver, the optical signal is filtered by a Gaussian filter with a bandwidth of 400 GHz. An electrical Bessel filter with a 70% of

the bit-rate bandwidth is used after the detection. The system performance is evaluated in terms of eye opening penalty (EOP) defined by $EOP = 10 \lg(EO_{b2b}/EO)$, where EO_{b2b} is the electrical eye opening in the case of back-to-back and EO is the electrical eye opening after fiber transmission. EOP is used to measure the distortions of an eye diagram for a worst case.

The nonlinear Schrödinger equation is solved by the split step Fourier method. The transmission line is composed of thirty 100-km spans and the loss is fully compensated by some noiseless erbium-doped fiber amplifiers (EDFAs). Neglecting the amplified spontaneous emission (ASE) noise allows focusing on the waveform distortions induced solely from intra-channel nonlinearity. Typical parameters of true wave reduced-slope (TWRS) fiber which is preferable in high-speed transmissions due to its low dispersion slope are used in the simulations: dispersion = 4.4 ps/(nm·km), dispersion slope = 0.045 ps/(km·nm²), $A_{eff} = 55 \mu\text{m}^2$, and $n_2 = 3.2 \times 10^{-20} \text{ m}^2/\text{W}$. The dispersion compensation fibers (DCFs) are inserted to solely compensate the second-order dispersion (SOD) leaving the cumulative TOD to the TOD

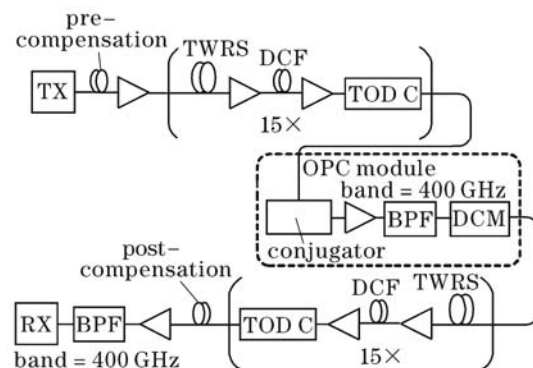


Fig. 1. Schematic diagram of the system configuration. TOD C: TOD compensator.

compensators. The tunable post-compensator is adjusted to make the net cumulative SOD at the end of the link be zero. TOD compensators are assumed to be an ideal element without loss, nonlinearity, and SOD. Although 160-Gb/s transmissions impose stringent demand on polarization-mode dispersion (PMD), many recent works have enabled advanced PMD monitoring and mitigation^[3,4], as well as a favorable PMD-resist property of fiber. In order to focus on the impact of chromatic dispersion and nonlinearities rather than PMD, neglecting PMD leads to the same simulation results with the case in which PMD is taken into account and has been appropriately compensated.

OPC module is located at the middle of transmission line. An ideal optical phase conjugator without wavelength conversion is used. The dispersion compensating module (DCM) in the OPC module is used to maintain the dispersion map because the optical phase conjugator inverts the sign of cumulative SOD of the signal^[2].

Dispersion mapping is the process of optimizing such parameters as residual SOD per span, pre- and post-compensation. In a link with a set of parameters: the number of spans N , the length of each span L , dispersion D , loss α and residual SOD per span D_{res} , the optimum pre-compensation value D_{pre} (ps/nm) is given by^[5]

$$\begin{aligned} D_{\text{pre}} &= -\frac{N \times D_{\text{res}}}{2} - \frac{D}{\alpha} \ln\left(\frac{2}{1 + e^{-\alpha L}}\right) \\ &= -\frac{15 \times D_{\text{res}}}{2} - 65.3, \end{aligned} \quad (1)$$

where 65.3 is obtained with the parameters: $D = 4.4$ ps/(nm·km), $\alpha = 0.2$ dB/km, and $L = 100$ km. The following optimized values in the simulations and the theoretical values show moderate agreement. For each case in the simulations, D_{res} is assumed to vary from 0 to 40 ps/nm with a step of 10 ps/nm and D_{pre} to vary with a step of 5 ps/nm to find their optimal values.

Considering a single optical pulse, the distortions induced by TOD can be compensated by a TOD-compensating element placed at any point of the link in linear regime^[6]. For an optical pulse train, the interactions between the adjacent pulses should be taken into account. Although the net cumulative TOD is compensated to zero at the end, the distortions of a pulse induced by nonlinear interactions with its neighboring pulses cannot be cancelled. These residual distortions can be explained by the intra-channel nonlinearity in pseudo-linear transmission systems. As shown in Fig. 2, it is simple to demonstrate the TOD effects only considering the propagation of a single pulse pair. Notice that the degree of the distortions illustrated in Fig. 2 is magnified to be observed obviously and the SOD is fully compensated in each point to focus on the TOD-solely-induced distortions. Due to the high bit rate of 160 Gb/s, the pulse profile is seriously distorted rapidly. Before full TOD compensation, the energy of a pulse leaks into the adjacent pulse whose phase is modulated by the magnitude fluctuations via Kerr effect and it generates timing and amplitude jitter. Considering two schemes of TOD compensation in Fig. 2, we verify the cumulative property of TOD-induced distortions. Comparing point E with point H in Fig. 2, larger cumulative TOD leads to the

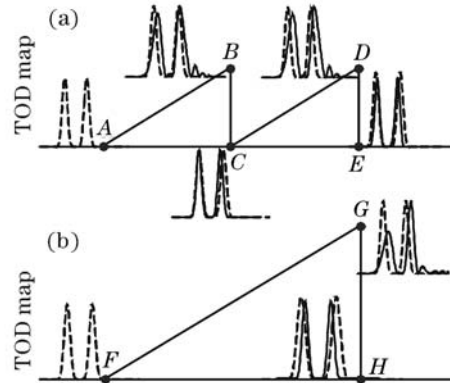


Fig. 2. Pictorial TOD maps and corresponding pulse evolution. (a) TOD compensation in each span; (b) TOD compensation only at the end.

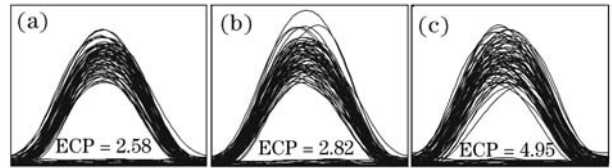


Fig. 3. Optical eye diagrams for RZ50 in 160-Gb/s 3000-km OPC systems with an input power of 7 dBm. (a) Neglecting TOD; (b) TOD compensation in each span; (c) TOD compensation only at the end.

increase in timing jitter. Accordingly, the scheme using TOD compensation in each span can mitigate the impact of TOD, as depicted at point E in Fig. 2. Although OPC combined with dispersion mapping can theoretically reduce the effects of intra-channel nonlinearity, the above arguments are also confirmed by the simulations for 160-Gb/s RZ50 OPC systems, as shown in Fig. 3. The input power is assumed to be 7 dBm (i.e. in nonlinear regime) and the optimized parameters are $D_{\text{res}} = 20$ ps/nm, and $D_{\text{pre}} = -360$ ps/nm. The scheme of using TOD compensation in each span (Fig. 3(b)) recovers the pulse profile effectively with about 2 dB improvement in eye closure penalty (ECP) compared with the scheme of only using TOD compensation at the end (Fig. 3(c)). ECP is well used to measure distortions of an eye diagram. Note that the distortions of the eye diagram in the absence of TOD (Fig. 3(a)) are attributed to the SOD-induced intra-channel nonlinearity.

According to the above discussion, both SOD and TOD can result in waveform distortions via intra-channel nonlinearities in nonlinear regime for high-speed transmissions. It has been shown that the system penalty due to intra-channel nonlinearity decreases with pulse-width shortening^[7]. This conclusion also holds in the OPC systems shown in Fig. 4 in terms of EOP as a function of the input power. A TOD-compensated transmission and a TOD-neglected transmission are taken into account where three modulation formats are simulated respectively. In each case, the values of D_{res} and D_{pre} have been optimized. In linear regime (i.e. low input power), all the modulation formats have approximately the same performance. Increase in input power leads to degradation of performance with a given threshold beyond which EOP increases rapidly due to intra-channel nonlinearity. Notice that when TOD is considered, there is an

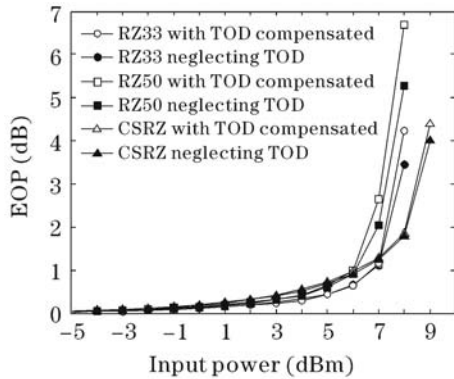


Fig. 4. EOP as a function of input power for three modulation formats in 160-Gb/s OPC systems after 3000-km transmission.

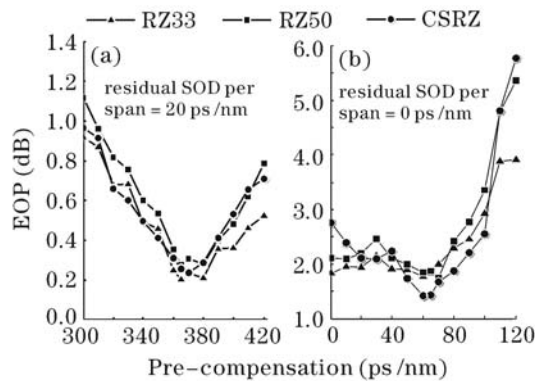


Fig. 5. Optimization of (a) pre-compensation for optimal residual SOD per span and (b) full compensation in each span in 160-Gb/s 3000-km OPC systems after TOD compensation. The input power is assumed to be 1 dBm.

obvious extra EOP beyond 6 dBm indicating TOD-induced distortions. RZ33 with smaller duty cycle outperforms RZ50 indicating its higher nonlinearity tolerance, while CSRZ with a 67% duty cycle is observed more resistant to the nonlinearity than RZ33 and RZ50 due to its π -phase-shift between adjacent pulses.

In addition to the above discussion on TOD effect, some simulations in 160-Gb/s TOD-compensated OPC systems involving dispersion mapping are carried out.

Figure 5 shows the optimization of dispersion map in terms of EOP as a function of pre-compensation. In each case, three modulation formats are investigated. Only the curves in optimized case (i.e. $D_{\text{res}} = 20$ ps/nm) are plotted (in Fig. 5(a)). The conventional scheme with full inline compensation (i.e. $D_{\text{res}} = 0$ ps/nm) exhibits tighter tolerance on a variation of pre-compensation especially beyond the optimal value. At optimal pre-compensation value, the scheme with optimized D_{res} makes a much more stable transmission due to its reduction of intra-channel nonlinearity^[2] (more than 1 dB improvement in EOP).

The estimations of SOD and TOD tolerances are also of great interest in optical transmission system designs. In the presence of residual SOD and TOD, Fig. 6 provides the curves at a given BER of 10^{-9} for the three modulation formats. According to the results, system tolerance on SOD and TOD can be mitigated by using modulation formats with a larger duty cycle (correspondingly a

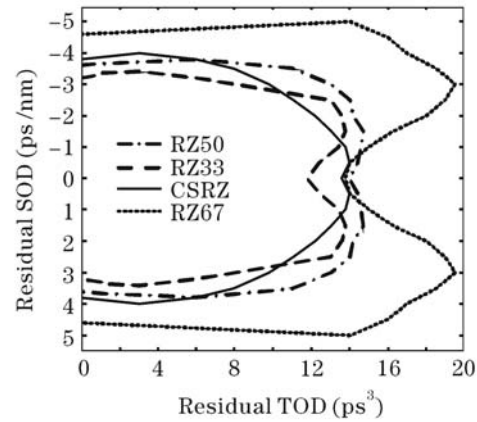


Fig. 6. SOD and TOD tolerance at BER = 10^{-9} in 160-Gb/s 3000-km OPC systems for various modulation formats, where the curve for normal RZ67 is also plotted so as to compare with CSRZ. The input power is 1 dBm.

narrower signal spectrum). However, CSRZ with a duty cycle of 67% does not agree with the rule due to its fixed phase difference between the adjacent pulses, compared with normal RZ67 (dotted in Fig. 6). Note that in the presence of some residual SOD with a range within ± 2 ps/nm, larger TOD tolerance can be obtained. Finally, comparing CSRZ from Fig. 4 and Fig. 6 shows its advantages in balancing system tolerances on intra-channel nonlinearity and chromatic dispersion.

In conclusion, intra-channel nonlinearity induced from TOD has been discussed with the help of numerical simulations. Considering dispersion mapping, performance comparison for three modulation formats in 160-Gb/s OPC systems was presented. The optimal dispersion map provides higher performance and lower sensitivity to the variation of pre-compensation, which indicates its validity in OPC systems. It is also shown that modulation formats with shorter duty cycle exhibit larger margin of the intra-channel nonlinearity but lower tolerance on chromatic dispersion. CSRZ could mitigate this conflict.

This work was supported by the National Natural Science Foundation of China under Grant No. 60577033. J Li's e-mail address is jqjlee@gmail.com.

References

1. C. Lorattanasane and K. Kikuchi, *J. Lightwave Technol.* **15**, 948 (1997).
2. A. Chowdhury, G. Raybon, R.-J. Essiambre, J. H. Sinsky, A. Adamiecki, J. Leuthold, C. R. Doerr, and S. Chandrasekhar, *J. Lightwave Technol.* **23**, 172 (2005).
3. L. Xi, X. Zhang, L. Yu, G. Zhou, H. Zhang, N. Zhang, J. Zhang, B. Wu, T. Yuan, M. Yao, and B. Yang, *Chin. Opt. Lett.* **2**, 262 (2004).
4. T. Li, M. Wang, C. Diao, and S. Jian, *Chin. Opt. Lett.* **2**, 138 (2004).
5. R. I. Killey, H. J. Thiele, V. Mikhailov, and P. Bayvel, *IEEE Photon. Technol. Lett.* **12**, 1624 (2000).
6. P. Kaewplung, T. Angkaew, and K. Kikuchi, *IEEE Photon. Technol. Lett.* **13**, 293 (2001).
7. A. Mecozzi, C. B. Clausen, and M. Shtaif, *IEEE Photon. Technol. Lett.* **12**, 1633 (2000).